Study on Optimal Layout of CO_2 Release Devices from the Perspective of Flow Field Dynamics in Greenhouses

Binnan WANG, Tingyi SHANG*

College of Information and Electrical Engineering, Heilongjiang Bayi Agricultural University, Daqing 163319, China

Abstract With the rapid development of modern agricultural technology, greenhouse facilities have become a cornerstone of agricultural production, and their application are becoming increasingly widespread. They play a significant role in enhancing agricultural productivity and crop quality. However, in practical application, particularly from morning to noon, the gradual increase in solar radiation intensifies the photosynthetic activity of plants inside greenhouses, leading to a significant rise in carbon dioxide consumption. This phenomenon not only reduces the concentration of carbon dioxide within greenhouses, but also limits the efficiency of photosynthesis to some extent, thereby adversely affecting the growth of greenhouse crops and potentially impacting the economic returns of agricultural production. To address this challenge, in this study, carbon dioxide release devices were introduced as a solution, and the effects of different placement positions of these devices on the distribution of carbon dioxide concentration within greenhouses were compared and analyzed applying analogue simulation methods. Through precise data collection and processing, this study aimed to determine the optimal placement position for carbon dioxide release devices to optimize the internal airflow distribution and enhance the utilization efficiency of carbon dioxide.

Key words Facility agriculture; Carbon dioxide; Simulation; Laminar flow

DOI:10.19759/j.cnki.2164 - 4993.2025.02.015

With the continuous development of facility agriculture, greenhouses, as critical production environments, rely heavily on the control of internal airflow distribution and carbon dioxide (CO_2) concentration for optimal crop growth. However, most greenhouse facilities still face limitations in environmental regulation, particularly in the selection of positions for CO_2 release devices, which directly impacts the flow field constraint law within greenhouses and the utilization efficiency of CO_2. Therefore, it is imperative to investigate the effects of different CO_2 release device positions on the flow field constraint law. It not only helps to improve the accuracy of environmental regulation, but also provides important reference for the design and optimization of greenhouse facilities, which is of great novelty and urgency[1].

The airflow distribution within any building is influenced by multiple factors, including its structure, ventilation methods, and layout[2], and greenhouses are no exception. As one of the key elements affecting airflow in greenhouses, the placement of CO_2 release devices can lead to variations in airflow patterns, thereby impacting the diffusion and distribution of CO_2[3]. Although numerous studies have been conducted at home and abroad on greenhouse environmental control and the application of CO_2 release devices, research on determining the optimal placement of these devices remains insufficient, lacking systematic theoretical analyses and experimental validation[4].

In recent years, foreign researchers have also made significant progress in this field. For example, Teitel *et al.*[5] combined simulation and experimental validation to investigate the impact of wind direction on air and crop temperatures in greenhouses, providing a theoretical basis for optimizing the placement of CO_2 release devices. Meanwhile, Takeshi Kuroyanagi *et al.*[6] studied the efficiency of CO_2 enrichment in unventilated greenhouses and proposed a strategy to effectively enhance yield while reducing CO_2 consumption, thereby improving CO_2 utilization efficiency. Additionally, Lamrani and Boulard[7] simulated free convection generated above plant canopies heated by solar radiation in real multi-span greenhouses from an engineering perspective, offering valuable recommendations for the design of CO_2 release systems. These studies by foreign researchers have not only enriched the knowledge in this field, but also provide critical references for subsequent research.

In addition to the aforementioned studies, numerous other foreign publications have offered important insights and support for this study. For instance, Cheng *et al.*[8] conducted a sensitivity analysis of factors influencing multi-zone indoor airflow, establishing a theoretical foundation for optimizing greenhouse design. Henten *et al.*[9] experimentally explored methods for enhancing greenhouse climate control efficiency within an optimal control theory framework, providing practical guidance for real-world applications. Furthermore, Ma and Carpenter *et al.*[10] investigated the relationship between microclimate conditions and crop growth in greenhouses, proposing novel approaches for environmental regulation.

To sum up, in this study, the research results at home and abroad were combined to thoroughly investigate the effects of different positions of CO_2 release devices on the flow field constraint law within greenhouses based on simulation modeling and experimental validation, aiming to provide a scientific basis for enhancing the precision of greenhouse environmental regulation and optimizing the design of greenhouse facilities.

Received: December 29, 2024 Accepted: February 27, 2025

Binnan WANG (2000 -), male, P. R. China, master, devoted to research about fluid mechanics, CFD simulation, and agricultural engineering.

* Corresponding author.

System Model

Continuity equation for fluid in greenhouses

The continuity equation for fluid inside a greenhouse describes the principle of mass conservation during the movement of the fluid. Since the mass of fluid inside a greenhouse cannot be created or vanish out of nowhere, it only flows from one part of the greenhouse to another.

The general form of the continuity equation for fluid inside a greenhouse can be expressed as:

$$\frac{\partial \rho}{\partial t} + \nabla \cdot (\rho u) = 0 \tag{1}$$

In the equation, ρ represents the density of the fluid inside the greenhouse, which is the mass of the fluid per unit volume; u denotes the velocity vector of the fluid, describing the speed of the fluid in various directions within the greenhouse; t represents time; $\frac{\partial}{\partial t}$ indicates the partial derivative with respect to time, describing the change in fluid density over time; ∇ is the differential operator, used to calculate gradients, divergences, and related parameter within the greenhouse; and $\nabla \cdot (\rho u)$ represents the spatial integral of the dot product of the fluid density and the velocity vector, which corresponds to the mass flow rate of the fluid inside the greenhouse.

With the continuity equation for fluid inside greenhouses, analyzing and predicting the flow behavior of fluid under different conditions becomes possible. It enables a more comprehensive description and analysis of the motion patterns of fluid within greenhouses.

Navier-Stokes equation

The Navier-Stokes equation describe the conservation of momentum for viscous fluid flow inside a greenhouse, reflecting the fundamental physical principles governing fluid motion within greenhouses. The equation holds an extremely important position in fluid mechanics and is widely applied in fields such as meteorology, oceanography, aerospace, and hydraulic engineering.

The form of the Navier-Stokes equation applicable to the fluid flow inside a greenhouse can be expressed as:

$$\rho\left(\frac{\partial u}{\partial t} + u \cdot \nabla u\right) = -\nabla p + \mu \nabla^2 u + f \tag{2}$$

In the equation, ρ represents the density of the fluid inside the greenhouse; u denotes the velocity vector of the fluid inside the greenhouse; t represents time; p represents the pressure of the fluid; μ denotes the dynamic viscosity coefficient of the fluid inside the greenhouse; and f represents the external body forces (such as gravity or electromagnetic forces) acting on the fluid inside the greenhouse; $\frac{\partial u}{\partial t}$ represents the change rate of the fluid velocity vector over time within the greenhouse, *i. e.*, accelerated velocity; $u \cdot \nabla u$ represents the convective term of the velocity vector of the fluid inside the greenhouse, describing the influence of velocity changes on momentum transport; $-\nabla p$ represents the effect of the pressure gradient on the fluid motion inside the greenhouse; and $\mu \nabla^2 u$ represents the viscous term, describing the effect of internal friction due to viscosity on the fluid motion inside the greenhouse.

The Navier-Stokes equation is essentially a set of vector equations. When expanded into the three coordinate axes (x, y, z) of the three-dimensional space of the greenhouse, they yield three component equations. These component equations describe the conservation of momentum of the fluid inside the greenhouse in the x, y, and z directions, respectively. The detailed forms of these three component equations are given below:

The Navier-Stokes equation in the x direction is:

$$\rho\left(\frac{\partial u}{\partial t} + u\frac{\partial u}{\partial x} + v\frac{\partial u}{\partial y} + w\frac{\partial u}{\partial z}\right) = -\frac{\partial u}{\partial x} + \mu\left(\frac{\partial^2 u}{\partial x^2} + \frac{\partial^2 u}{\partial y^2} + \frac{\partial^2 u}{\partial z^2}\right) + f_x \tag{3}$$

The Navier-Stokes equation in the y direction is:

$$\rho\left(\frac{\partial v}{\partial t} + u\frac{\partial v}{\partial x} + v\frac{\partial v}{\partial y} + w\frac{\partial v}{\partial z}\right) = -\frac{\partial p}{\partial y} + \mu\left(\frac{\partial^2 v}{\partial x^2} + \frac{\partial^2 v}{\partial y^2} + \frac{\partial^2 v}{\partial z^2}\right) + f_y \tag{4}$$

The Navier-Stokes equation in the z direction is:

$$\rho\left(\frac{\partial w}{\partial t} + u\frac{\partial w}{\partial x} + v\frac{\partial w}{\partial y} + w\frac{\partial w}{\partial z}\right) = -\frac{\partial p}{\partial z} + \mu\left(\frac{\partial^2 w}{\partial x^2} + \frac{\partial^2 w}{\partial y^2} + \frac{\partial^2 w}{\partial z^2}\right) + f_z \tag{5}$$

In the equation, ρ represents the density of the fluid inside the greenhouse; u, v and w denote the velocity components of the fluid in the x, y, and z directions, respectively; t represents time; p is the pressure within the fluid inside the greenhouse; μ is the dynamic viscosity coefficient of the fluid; and f_x, f_y, and f_z are the components of the external body forces acting on the fluid in the x, y, and z directions, respectively.

These component equations describe the momentum changes of the fluid inside the greenhouse in each direction within the three-dimensional space, as well as how these changes are influenced by pressure gradients, viscous forces, and external body forces.

Convection-diffusion equation for exterior space of greenhouses

Since the interior space of a greenhouse is a three-dimensional volume, the three-dimensional convection-diffusion equation is applicable to this scenario. The convection-diffusion equation for the interior space of a greenhouse is a mathematical model that describes the transport of fluid components within the greenhouse due to convection and diffusion. As carbon dioxide release devices are placed inside the greenhouse, the interaction between the internal air and the carbon dioxide released by these devices leads to convection and diffusion.

The convection-diffusion equation for the interior space of a greenhouse can be expressed as:

$$\frac{\partial C}{\partial t} + u \cdot \nabla C = D \nabla^2 C \tag{6}$$

In the equation, C represents the concentration of the substance; t denotes time; u is the velocity vector of the fluid inside the greenhouse, composed of three components u, v, and w, corresponding to the velocities in the w, y, and z directions, respectively; ∇ is the gradient operator, representing the rate of change in the interior space of the greenhouse; D is the diffusion

coefficient, describing the rate at which the fluid components diffuse within the space; and ∇^2 is the Laplacian operator, representing the second-order spatial derivative, used to describe the diffusion process of the fluid components inside the greenhouse.

Turbulence model for fluid inside greenhouses

The $k-\varepsilon$ model was used in this study. The $k-\varepsilon$ model is one of the most widely used turbulence models in the research of fluid dynamics, primarily employed to describe the turbulent kinetic energy k and the turbulent kinetic energy dissipation rate ϵ of the turbulent flow inside greenhouses. The basic assumption of the $k-\varepsilon$ model used in this study was that the turbulent kinetic energy in the turbulent flow inside greenhouses is the same in all directions, that is, the turbulence is isotropic, and the dissipation rate of the turbulent kinetic energy is proportional to the square of the turbulent kinetic energy. The equations of the $k-\varepsilon$ model for the interior fluid of a greenhouse include two main transport equations:

(1) The transport equation for turbulent kinetic energy k of the turbulence in the greenhouse:

$$\frac{\partial(\rho k)}{\partial t}+\frac{\partial(\rho k u_i)}{\partial x_i}=\frac{\partial}{\partial x_i}\left[\left(\mu+\frac{\mu_t}{\sigma_k}\right)\frac{\partial k}{\partial x_j}\right]+P_k-\rho\varepsilon \tag{7}$$

In the equation, ρ represents the density of the fluid inside the greenhouse; u_i denotes the velocity component of the fluid in the i direction; μ is the dynamic viscosity of the fluid inside the greenhouse; μ_t is the turbulent viscosity of the fluid inside the greenhouse, typically expressed as a function of k and ϵ; σ_k is the Prandtl number corresponding to the turbulent kinetic energy of the turbulence in the greenhouse; P is the production term of turbulent kinetic energy, usually related to the mean velocity gradient of the fluid inside the greenhouse and the turbulent viscosity inside the greenhouse; and ϵ is the dissipation rate of turbulent kinetic energy inside the greenhouse.

(2) The transport equation for the turbulent kinetic energy dissipation rate ϵ of the turbulence in the greenhouse:

$$\frac{\partial(\rho\varepsilon)}{\partial t}+\frac{\partial(\rho\varepsilon u_i)}{\partial x_i}=\frac{\partial}{\partial x_j}\left[\left(\mu+\frac{\mu_i}{\sigma_\varepsilon}\right)\frac{\partial\varepsilon}{\partial x_j}\right]+C_{\varepsilon 1}\frac{\varepsilon}{k}P_k-C_{\varepsilon 2}\rho\frac{\varepsilon^2}{k} \tag{8}$$

In the equation, σ_ε is the Prandtl number corresponding to the dissipation rate of turbulent kinetic energy; and $C_{\varepsilon 1}$ and $C_{\varepsilon 2}$ are empirical constants, typically assigned standard values.

For the $k-\varepsilon$ model employed in this study, the spatial distributions of turbulent kinetic energy (k) and its dissipation rate (ϵ) within the greenhouse were calculated by solving these two transport equations. Further, the computation of turbulent viscosity u_i inside the greenhouse was enabled, thereby realizing the simulation of turbulent flow inside the greenhouse.

Heat transfer equation for fluid inside greenhouses

In this study, the heat transfer equation for the fluid inside greenhouses was mainly used to describe the heat transfer process between the air in the greenhouses and surrounding structures (such as walls and roofs). The heat transfer mechanisms within greenhouses mainly involve three fundamental modes: convection, radiation, and conduction. These processes are jointly influenced by both internal environmental parameters (such as temperature, humidity and air velocity) and external climatic conditions (such as solar radiation and ambient temperature).

Considering these factors, the heat transfer equation for the fluid inside a greenhouse in this study took the following form:

$$\rho c_p\frac{\partial T}{\partial t}+\rho c_p u\cdot\nabla T=\nabla\cdot(K\nabla T)+Q_{rad}+Q_{cond} \tag{9}$$

In the equation, ρ represents the density of the fluid inside the greenhouse; c_p denotes the specific heat capacity for the fluid inside the greenhouse; T is the temperature of the fluid inside the greenhouse; t represents time; u is the velocity vector for the fluid inside the greenhouse; ∇T indicates the temperature gradient of the fluid inside the greenhouse; k is the thermal conductivity coefficient of the fluid inside the greenhouse; Q_{rad} represents the heat source term caused by radiative heat transfer; and Q_{cond} is the heat source term resulting from conductive heat transfer.

The above equation describes the temporal variation of fluid temperature inside the greenhouse and the heat transfer caused by convection, radiation, and conduction. The left-hand side of the equation represents the temperature change over time and the heat transfer caused by conduction within the greenhouse, while the right-hand side represents the heat transfer caused by heat conduction, radiation, and conduction.

Simulation Results of Experimental Data

Experimental greenhouse model

In this study, the effects of different placement positions of CO_2 release devices on the flow field constraint law inside greenhouses under specific climatic conditions in Daqing City, Heilongjiang Province (46° N, 125° E) in April were investigated. The greenhouses were covered with single-layer polyethylene plastic film and exhibited distinct structural characteristics, specifically: a span of 10 m in the north-south direction, a height of 4.3 m, and a length of 110 m in the east-west direction. In particular, this study focused on analyzing the specific effects of different CO_2 release point layouts on the internal flow field data of the greenhouses. The arrangement and operational scenarios of a CO_2 release device in an actual greenhouse are illustrated in Fig. 1. Through in-depth analysis of these data, this study aimed to provide a scientific basis for optimizing the environment management inside greenhouses.

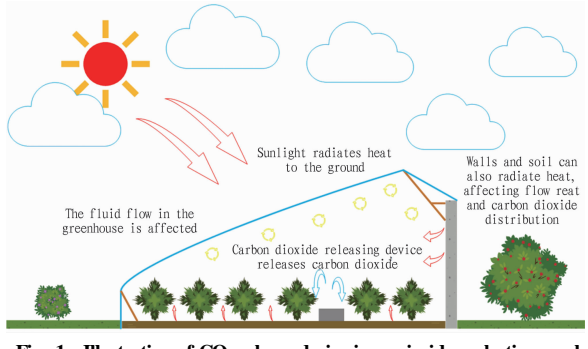

Fig. 1 Illustration of CO_2 release device in use inside a plastic greenhouse

To thoroughly explore the optimal placement for CO_2 release devices within greenhouses, three distinct placement schemes were designed meticulously in this study. First, in the initial scheme, a 1 m × 1 m CO_2 release device was positioned 55 m away from the east wall and 0.5 m away from the gable wall of the greenhouse. Second, in the second scheme, the release device was positioned at the same distance of 55 m away from the east wall, but 4.5 m away from the gable wall. Finally, the third scheme involved placing a CO_2 release device of the same size 36 m away from the east wall and 0.5 m away from the gable wall. This study aimed to reveal the specific impact of the placement position of CO_2 release devices on the flow field constraint law by comparing the changes in the velocity field and the CO_2 concentration within sealed greenhouses under these different schemes. These flow field data were analyzed in detail and systematically to more accurately evaluate the effectiveness of each placement scheme and determine the optimal configuration. Additionally, for clarity and reference, Fig. 2 provides a three-dimensional diagram of the sealed greenhouse used in this experiment, showing the structure and dimensions of the greenhouse as well as the potential placement positions of CO_2 release devices. Through these detailed experimental designs and data analyses, this study aimed to provide scientific theoretical support and guidance for greenhouse management practice.

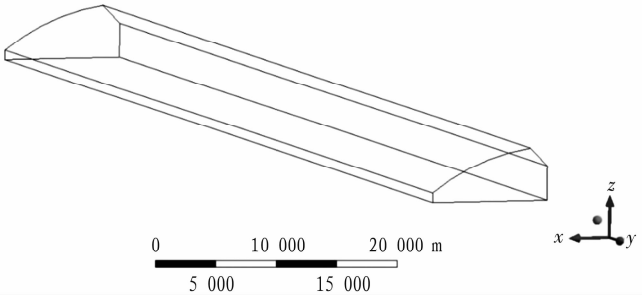

Fig. 2 Three-dimensional perspective view of a sealed plastic greenhouse

In this study, to thoroughly investigate the impact of the placement position of CO_2 release devices on the flow field constraint law within greenhouses, the widely-recognized Ansys Fluent software was employed for numerical simulation analysis. To ensure the accuracy and authenticity of the simulation results, local climate and geographical data from Daqing City, Heilongjiang Province, were incorporated as input parameters, so as to more accurately reflect the actual local conditions. For a comprehensive analysis on the impact of CO_2 release device positions on the flow field, the SIMPLEC algorithm was selected due to its exceptional performance in solving pressure-linked equations. Known for its efficiency and stability, the SIMPLEC algorithm not only significantly improved the convergence speed of simulation, but also enhanced the accuracy of the results, providing robust support for the in-depth analysis of the flow field constraint law. To facilitate subsequent academic discussion and presentation of findings, the numbering method illustrated in Fig. 3 was adopted to identify different CO_2 release positions within greenhouses. Specifically, greenhouse 1 represents the CO_2 release device positioned 55 m away from the east wall and 0.5 m away from the gable wall. Greenhouse 2 represents the device positioned 55 m away from the east wall and 4.5 m away from the gable wall. And greenhouse 3 represents the device positioned 36 m away from the east wall and 0.5 m away from the gable wall. Such numbering method not only aided in clearly describing the positions of the CO_2 release devices, but also provided a definitive reference for subsequent analysis on the flow field constraint law.

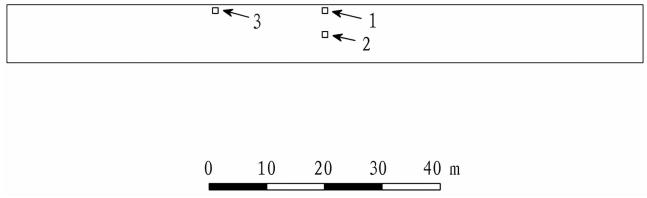

Fig. 3 Location map of carbon dioxide release devices in closed plastic greenhouses

Velocity field variation in greenhouses under normal light conditions

Through a detailed analysis of velocity field for different placement positions of carbon dioxide release devices, significant changes in the flow field constraint law were observed. These changes were not only reflected in the noticeable differences in airflow velocity and the variability in flow direction, but also profoundly affected the spatial distribution uniformity of carbon dioxide concentration inside greenhouses.

The three images in Fig. 4 visually illustrate the flow field distribution generated by carbon dioxide release devices placed at different locations inside the greenhouses under normal light conditions. Firstly, for greenhouse 1 (with the carbon dioxide release device located 55 m away from the east wall and 0.5 m away from the gable wall), the velocity streamline diagram reveals a relatively chaotic flow pattern within the flow field, accompanied by a distinct red high-speed region near the release device, which indicated that carbon dioxide tended to accumulate in the region, making it difficult to diffuse effectively throughout the greenhouse space, potentially reducing the utilization efficiency of carbon dioxide. In contrast, the streamline diagram of greenhouse 2 shows smoother streamlines and more uniform color distribution, indicating a more reasonable velocity distribution within the greenhouse. The layout facilitated the even diffusion of carbon dioxide, thereby improving its utilization efficiency within the greenhouse and positively impacting plant growth. As for greenhouse 3 (with the carbon dioxide release device located 36 m away from the east wall and 0.5 m away from the gable wall), its streamline diagram displays relatively regular streamlines, but it is evident that the velocity is higher near the release device and lower in other areas of the greenhouse. Such uneven velocity distribution might lead to an uneven distribution of carbon dioxide within the greenhouse, affecting the photosynthetic efficiency of the plants. In summary, the placement of the carbon dioxide release device in greenhouse 2 ensured effective diffusion of carbon dioxide while avoiding excessive concentration in localized areas, providing a more ideal growth environment for the plants inside the greenhouse.

To more precisely analyze the velocity variation characteristics inside different greenhouses, this study selected three representative monitoring points, each located at a specific position within the greenhouses. These monitoring points were as follows: the first point located 5 m away from the gable wall and 5 m away from the east wall, at a height of 1 m above the ground, the second point located 5 m away from the gable wall and 55 m away from the east wall, also at a height of 1 m above the ground, and the third point located 5 m away from the gable wall and 109 m away from the east wall, again at a height of 1 m above the ground. Corresponding velocity variation diagrams were plotted (Fig. 5 – Fig. 7) by continuously monitoring the velocity changes at these three points over a period of 3 h. These detailed data and charts provide profound insights into the velocity variation patterns inside different greenhouses, facilitating further understanding and optimizing airflow management and environmental control strategies within greenhouses.

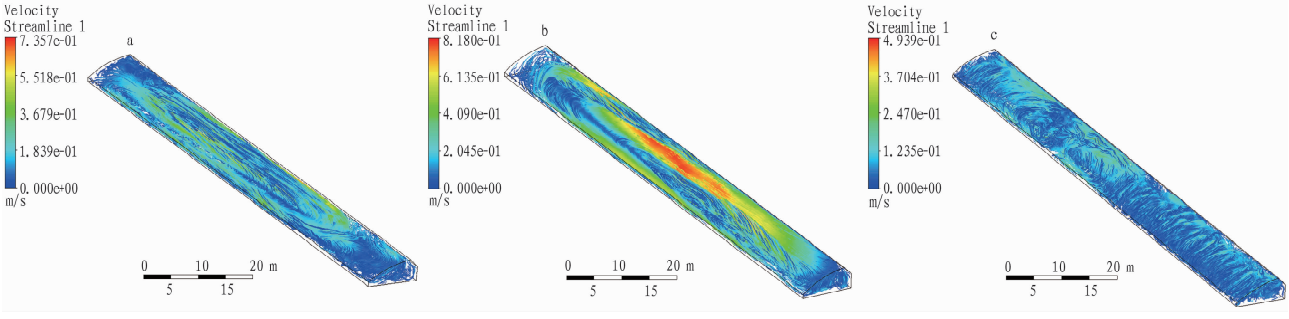

Fig. 4 Diagrams of velocity streamlines inside greenhouses (a: greenhouse 1, b: greenhouse 2, c: greenhouse 3)

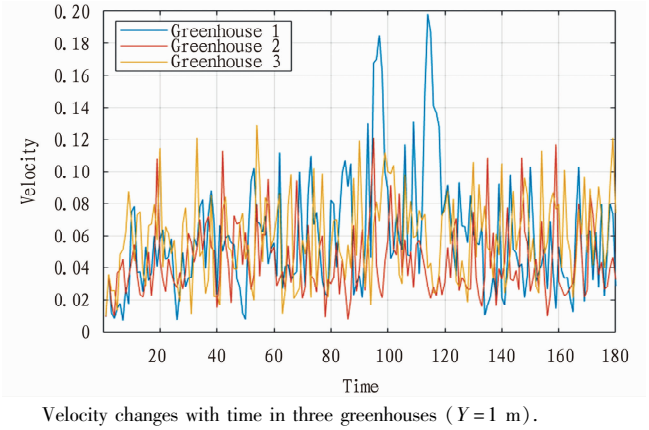

Velocity changes with time in three greenhouses (Y = 1 m).

Fig. 5 Changes of velocity at the point 5 m away from the gable wall of the greenhouse, 5 m from the east wall of the greenhouse and 1 m away from the ground

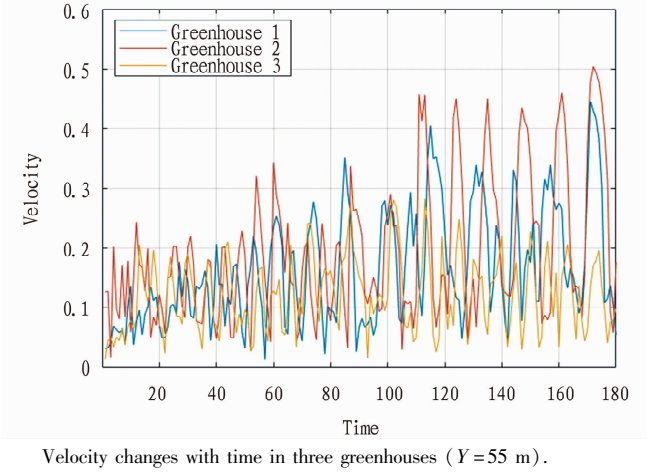

Velocity changes with time in three greenhouses (Y = 55 m).

Fig. 6 Changes of velocity at the point 5 m away from the gable wall of the greenhouse, 55 m from the east wall of the greenhouse and 1 m away from the ground

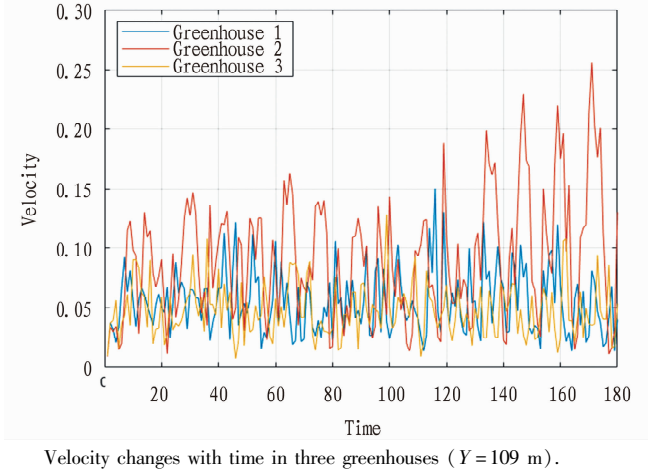

Velocity changes with time in three greenhouses (Y = 109 m).

Fig. 7 Changes of velocity at the point 5 m away from the gable wall of the greenhouse, 109 m from the east wall of the greenhouse and 1 m away from the ground

The analysis results indicated that the velocity variation characteristics at the monitoring point located 1 m away from the east wall of the greenhouse were significant. Due to its proximity to both the gable wall and the east wall, the airflow inside the greenhouse was subject to multiple constraints at this point, resulting in considerable velocity fluctuations. Particularly when greenhouse ventilation was restricted or light intensity changed, the velocity variations at this point were especially pronounced. In contrast, the monitoring point located 55 m away from the east wall, being relatively central and maintaining a certain distance from the east, west, and gable walls, exhibited more stable airflow and more gentle velocity changes. This finding suggests that in more central locations within greenhouses, airflow is less affected by boundary effects, thereby facilitating the maintenance of relatively constant environmental conditions. Finally, at the monitoring point located 1 m away from the west wall (*i. e.*, 109 m away from the east

wall), the airflow was significantly obstructed by the west wall, leading to relatively larger velocity variations. This result further confirms that the airflow characteristics inside greenhouses are importantly influenced by boundary conditions. In summary, these findings contribute to optimizing greenhouse design and environmental control strategies to achieve higher plant growth efficiency and yield.

To delve deeper into the specific impact of carbon dioxide release on the velocity distribution inside greenhouses, in this study, an average of 1 000 points on cross-sections located 1, 55, and 109 m away from the east wall at a height of 1 m above the ground were also selected. The averages, medians and standard deviations of the velocity values at these points were analyzed, and the resulting data are presented in Table 1.

Table 1 Descriptive statistical data of velocity at 1 m above ground level and 109 m away from the east wall in the three greenhouses

Location of cross-section	Greenhouse No.	Mean//m/s	Median//m/s	Standard deviation
1 m away from the the east wall, 1 m above the ground	Greenhouse 1	0.058 0	0.054 0	0.026 3
	Greenhouse 2	0.031 8	0.030 4	0.014 1
	Greenhouse 3	0.035 5	0.034 1	0.011 8
55 m away from the the east wall, 1 m above the ground	Greenhouse 1	0.238 4	0.193 5	0.166 0
	Greenhouse 2	0.347 3	0.310 0	0.177 3
	Greenhouse 3	0.062 8	0.053 0	0.025 9
109 m away from the the east wall, 1 m above the ground	Greenhouse 1	0.031 8	0.032 9	0.008 8
	Greenhouse 2	0.083 8	0.087 4	0.036 9
	Greenhouse 3	0.041 7	0.044 7	0.012 7

Table 1 reveals that the means, medians, and standard deviations of wind speed varied across different greenhouses and cross-sectional positions. The distribution of wind speed within greenhouses affects the diffusion and mixing of carbon dioxide, thereby influencing the uniformity of carbon dioxide distribution. In terms of the mean value, at the three different cross-sectional positions (1, 55 and 109 m away from the east wall), greenhouse 2 exhibited the highest average velocity values, indicating that, under the same conditions, the overall velocity within greenhouse 2 was higher. For carbon dioxide distribution, higher velocities facilitate gas mixing and distribution, ensuring uniform carbon dioxide concentration within greenhouses. Regarding the median value, greenhouse 2 also showed relatively higher medians, consistent with its mean values. In terms of the standard deviation, at the 1 and 109 m positions, greenhouse 2 had relatively lower standard deviations, further indicating a more uniform velocity distribution within greenhouse 2. In summary, the wind speed distribution in greenhouse 2 was most conducive to the uniform distribution of carbon dioxide. The higher wind speeds and relatively lower standard deviations meant that carbon dioxide in greenhouse 2 could be mixed and distributed more quickly throughout the greenhouse, thereby reducing local variations in carbon dioxide concentration.

To precisely quantify the effects of carbon dioxide release devices on airflow distribution within greenhouses and optimize their placement positions accordingly, the airflow velocities at specific cross-sections within the greenhouses were systematically measured and analyzed in this study. Specifically, three representative cross-sections located 1, 55 and 109 m away from the east wall were selected, and detailed velocity data were collected at a height of 1 m above the ground on each cross-section. To gain deeper insights into the characteristics of these datasets, the cumulative distribution function (CDF) was further applied for analysis, as shown in Fig. 8 to Fig. 10, so as to provide a comprehensive assessment of the effects of different carbon dioxide release device placements on airflow distribution.

As shown in Fig. 8 to Fig. 10, the velocity data within the greenhouses exhibited a significant increasing trend over time, reflecting the positive impact of carbon dioxide release on fluid dynamics. Further analysis revealed notable differences in the characteristics of fluid velocity changes inside the greenhouses. In particular, the fluid velocity in greenhouse 2 tended to be stable after a short decline in the initial stage, and the velocity changes were no longer significant after a certain distance, indicating that the environmental conditions within greenhouse 2 were more balanced and stable and facilitated the uniform diffusion of carbon dioxide. In contrast, the fluid velocity changed more sharply in greenhouses 1 and 3, which might lead to uneven distribution of fluid components, thus affecting the efficiency of plant utilization of carbon dioxide. In summary, the variations in fluid velocity inside the greenhouses were affected not only by carbon dioxide release, but also by a combination of environmental conditions and fluid dynamics characteristics.

Carbon dioxide release in the greenhouses under normal light conditions

Under normal light conditions, the efficiency of carbon dioxide release devices placed at different locations within the greenhouses was investigated thoroughly in this study. The results showed that the distribution of carbon dioxide within the greenhouses was significantly affected by airflow speed and direction, while the uniformity of carbon dioxide concentration inside the greenhouses was also a critical consideration factor. This finding is crucial for understanding the mechanisms of greenhouse environmental control and optimizing carbon dioxide release strategies, and provides valuable references for subsequent research. Fig. 11 shows the mass fraction distribution of carbon dioxide 3 h after its release by the carbon dioxide release devices under normal light conditions.

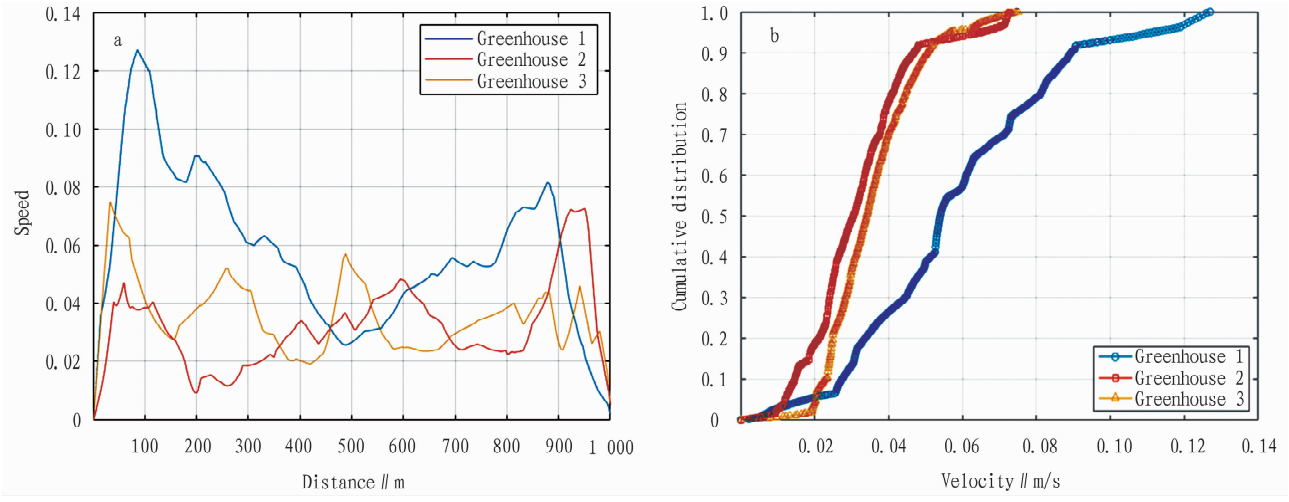

a. 1 m away from the east wall and 1 m away from the ground; b. Cumulative distribution function of velocity data (Y = 1 m).

Fig. 8 Diagrams of velocity distribution and cumulative distribution function at 1 m away from the east wall of the greenhouse

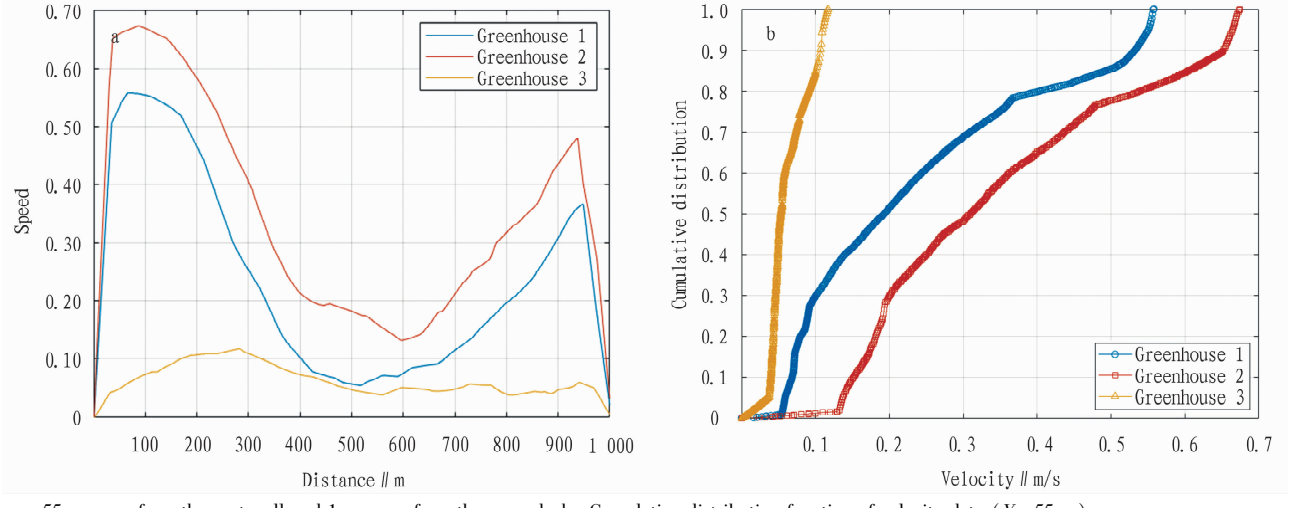

a. 55 m away from the east wall and 1 m away from the ground; b. Cumulative distribution function of velocity data (Y = 55 m).

Fig. 9 Diagrams of velocity distribution and cumulative distribution function at 55 m away from the east wall of the greenhouse

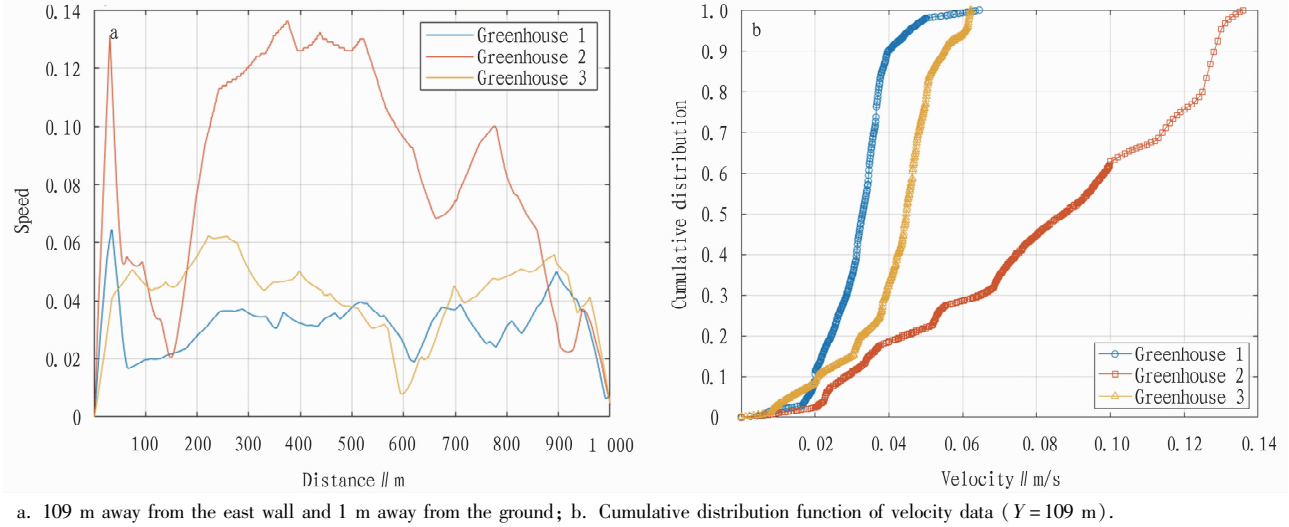

a. 109 m away from the east wall and 1 m away from the ground; b. Cumulative distribution function of velocity data (Y = 109 m).

Fig. 10 Diagrams of velocity distribution and cumulative distribution function at 109 m away from the east wall of the greenhouse

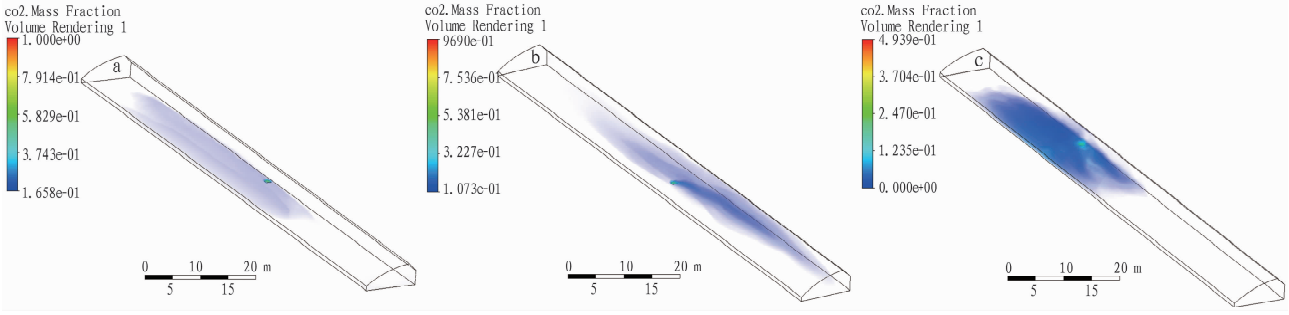

Fig. 11 Diagrams of carbon dioxide mass fraction inside the greenhouses (a: greenhouse 1, b: greenhouse 2, c: greenhouse 3)

Through the analysis of carbon dioxide mass fraction diagrams with different placement positions, it could be concluded that in greenhouse 1, the carbon dioxide mass fraction near the carbon dioxide release device was significantly higher, but the distribution of carbon dioxide was uneven during airflow diffusion. The concentration of carbon dioxide was higher in regions close to the gable wall and lower in regions farther from the gable wall. This unevenness might be due to the blocking effect of the gable wall on the internal airflow, making it difficult for carbon dioxide to diffuse uniformly throughout the greenhouse space. In contrast, the distribution of carbon dioxide in greenhouse 2 was more uniform. It was because the carbon dioxide release device was located farther from the gable wall, and reduced the blocking effect of the wall on airflow, thereby promoting uniform diffusion of carbon dioxide within the greenhouse. In greenhouse 3, the distribution of carbon dioxide showed a clear gradient. The concentration was high near the carbon dioxide release device and lower in regions farther from the device. The gradient might be due to the proximity of the release device to the east wall, which affected the internal airflow and limits the diffusion range of carbon dioxide. In summary, the uniform diffusion of carbon dioxide was closely related to the placement positions of carbon dioxide release devices. A reasonable placement strategy can significantly improve the uniformity of carbon dioxide distribution within greenhouses, thereby enhancing the photosynthetic efficiency and yield of plants.

The placement positions of carbon dioxide release devices have a significant impact on the uniformity of carbon dioxide distribution within greenhouses. To achieve more uniform carbon dioxide distribution, release devices should be placed away from the walls of greenhouses to reduce the blocking effect of the walls on airflow. Based on the airflow characteristics within greenhouses and the growth requirements of crops, it is recommended to place the carbon dioxide release devices in the center or slightly off center of the greenhouses to ensure that carbon dioxide can diffuse uniformly throughout the greenhouse spaces. In this regard, the placement

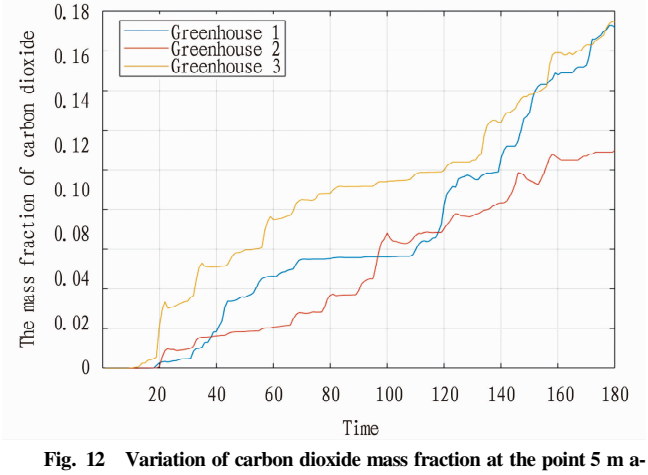

Fig. 12 Variation of carbon dioxide mass fraction at the point 5 m away from the gable wall, 5 m away from the east wall and 1 m above the ground (Y=1 m)

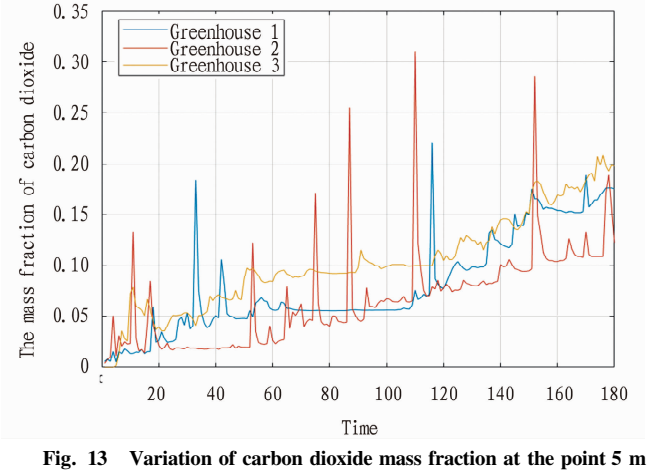

Fig. 13 Variation of carbon dioxide mass fraction at the point 5 m away from the gable wall, 55 m away from the east wall and 1 m above the ground (Y=55 m)

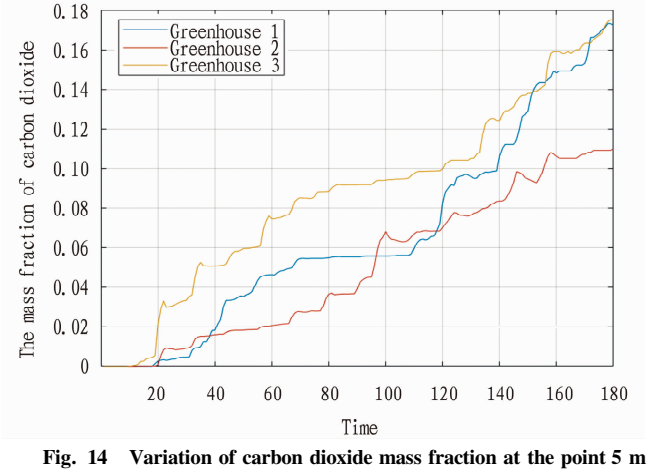

Fig. 14 Variation of carbon dioxide mass fraction at the point 5 m away from the gable wall, 109 m away from the east wall and 1 m above the ground (Y=109 m)

strategy of greenhouse 2 was particularly suitable, as it achieved a high degree of uniform carbon dioxide diffusion, providing an effective reference for greenhouse environmental regulation.

To study the dynamic changes of carbon dioxide components inside greenhouses in detail, in this study, three representative points were selected and continuously monitored for the mass fraction of carbon dioxide over a three-hour period. One of the points was located at 5 m away from the gable wall, 5 m away from the east wall, and 1 m above the ground. Another one was located at 5 m away from the gable wall, 55 m away from the east wall, and 1 m above the ground. The last one was located at 5 m away from the gable wall, 109 m away from the east wall, and 1 m above the ground. Through analysis on the monitoring data from these points, the trends of carbon dioxide concentration changes over time at different locations were revealed, as shown in Fig. 12 to Fig. 14.

Fig. 12 to Fig. 14 show that although the carbon dioxide mass fraction fluctuated over time, it generally exhibited an increasing trend, indicating that certain constraints within the greenhouses caused local accumulation of carbon dioxide. Comparing greenhouses 1 and 3, despite both being close to the gable wall, the trends in carbon dioxide mass fraction changes were similar, suggesting that the position of the east wall had a smaller impact on carbon dioxide diffusion, while the distance from the gable wall was a key influencing factor. In contrast, the carbon dioxide mass fraction in greenhouse 2 showed smaller and more stable changes, indicating that when the release device was farther from the gable wall, the diffusion of carbon dioxide was more uniform and less constrained. Therefore, the placement position of release devices is crucial for improving the distribution of carbon dioxide, and positions farther from the gable wall help achieve more uniform carbon dioxide distribution.

To thoroughly investigate the distribution characteristics of carbon dioxide within greenhouses, in this study, two horizontal planes at distances $X = 4$ and $X = 7$ from the gable wall were selected for in-depth analysis. The analysis results are shown in Fig. 15 and Fig. 16, respectively.

Through comparison on the contour maps of carbon dioxide mass fractions at different locations, it was found that the placement positions of carbon dioxide release devices significantly affected the distribution of carbon dioxide inside the greenhouses in this study. Specifically, when the release device was located 55 m away from the east wall and 0.5 m away from the gable wall, carbon dioxide primarily flowed toward the center and northern parts of the greenhouse, with a relatively uniform distribution. However, premature deposition of carbon dioxide near the gable wall was observed, which might adversely affect plant growth. In contrast, when the distance between the release device and the gable wall was increased to 4.5 m, the flow of carbon dioxide became more extensive, covering almost the entire greenhouse, and the deposition near the gable wall was significantly reduced, indicating improved uniformity in carbon dioxide distribution. Further observation of the carbon dioxide distribution when the release device was located 36 m away from the east wall and 0.5 m away from the gable wall showed that, despite the reduced distance from the east wall, significant deposition near the gable wall was still remarkable. It further underscored the importance of the distance between carbon dioxide release devices and the gable wall for achieving uniform carbon dioxide distribution. In summary, the placement positions of carbon dioxide release devices in the greenhouses significantly influenced the flow field constraint law. To improve carbon dioxide distribution, it is recommended to appropriately increase the distance between carbon dioxide release devices and the gable wall and consider the overall structure and ventilation conditions of greenhouses to ensure that carbon dioxide can diffuse uniformly throughout the greenhouses, providing an optimal growth environment for crops.

To comprehensively reveal the dynamic changes in carbon dioxide mass fraction inside the greenhouses and visually demonstrate the impact of carbon dioxide release devices' position on the uniformity of carbon dioxide distribution, this study introduced the concept of carbon dioxide uniformity. The standard deviation and average of these concentrations were calculated by measuring carbon dioxide concentration at multiple locations and different time within the greenhouses, and then, a percentage was obtained by dividing the standard deviation by the average, deriving a specific numerical value. The smaller the value, the more uniform the carbon dioxide distribution, and the more favorable the carbon dioxide environment within the greenhouse for crop growth. In this study, the data of changes in carbon dioxide concentration were randomly collected from 15 points at or below 1 m above the ground, and the carbon dioxide uniformity within the greenhouses were calculated based on this algorithm, as shown in Table 2.

Table 2 Carbon dioxide uniformity in the three greenhouses at different time

Position of cross-section	1 h	2 h	3 h
Greenhouse 1	93.885 291%	82.821 832%	98.595 678%
Greenhouse 2	72.202 113%	95.276 774%	96.422 438%
Greenhouse 3	84.481 383%	83.018 953%	86.693 898%

Based on the content in Table 2, it can be observed that when carbon dioxide was released for 1 h, the carbon dioxide uniformity in greenhouse 2 was 72.202 113%. Although this value was the lowest among the three greenhouses, it was not too low considering that the carbon dioxide concentration was not as high as possible, but needed to be kept in a suitable range to promote plant growth. Over the next 2 h, the carbon dioxide uniformity in greenhouse 2 significantly increased to 95.276 774%, a value that not only exceeded those of greenhouses 1 and 3 at the same time point but also demonstrated the excellent uniformity of carbon dioxide distribution in greenhouse 2. To the point of 3 h, the carbon dioxide uniformity in greenhouse 2 remained at a high level of 96.422 438%, further proving the rationality of the placement position of its carbon dioxide release device. In contrast, the carbon dioxide uniformity in greenhouse 1 was the highest within 1 h but significantly decreased over the next 2 h, indicating unstable carbon dioxide distribution. Meanwhile, the carbon dioxide uniformity in greenhouse 3 was relatively consistent across the three time points but did not reach the high level of uniformity observed in greenhouse 2.

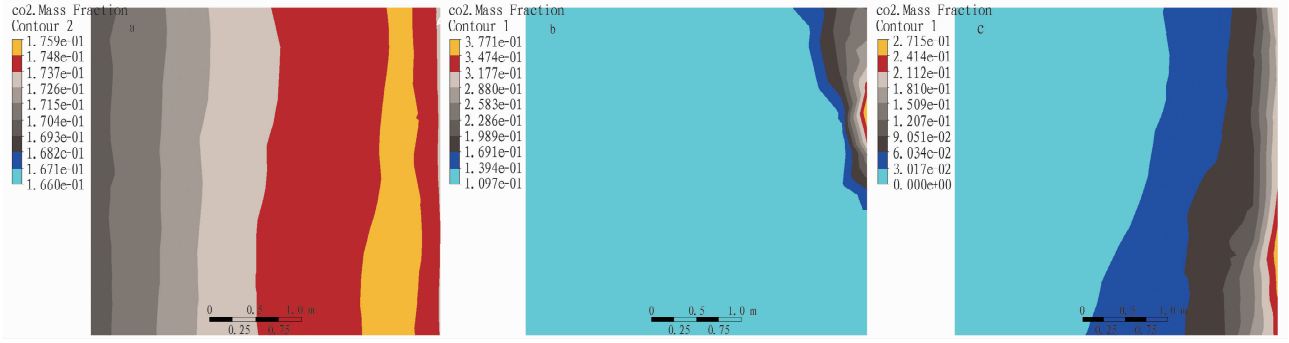

Fig. 15 Cloud maps of carbon dioxide mass fraction at 4 m away from the gable wall in the greenhouses (a: greenhouse 1, b: greenhouse 2, c: greenhouse 3)

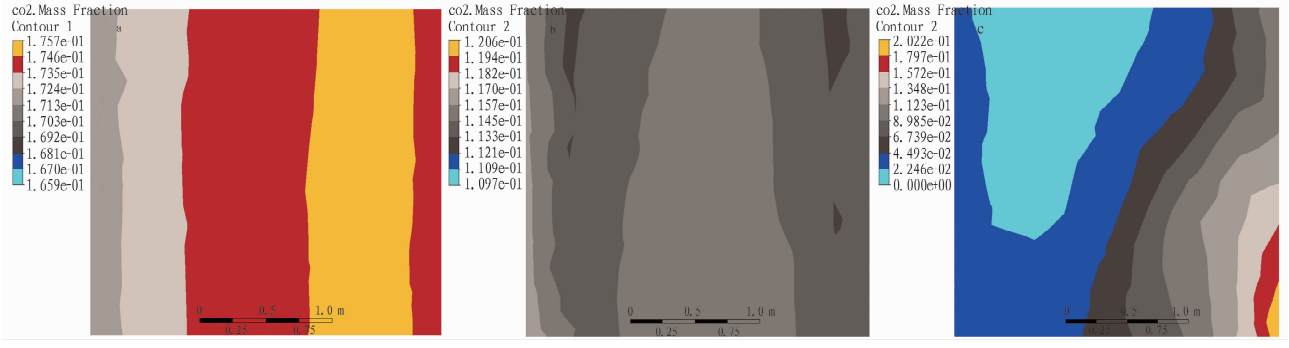

Fig. 16 Cloud maps of carbon dioxide mass fraction at 7 m away from the gable wall in the greenhouses (a: greenhouse 1, b: greenhouse 2, c: greenhouse 3)

To more accurately assess the uniformity of carbon dioxide distribution inside the greenhouses, three representative points at different locations were further selected within the three greenhouses in this study (point 1: 1 m away from the east wall, 1 m away from the gable wall, and 0.5 m above the ground; point 2: 45 m away from the east wall, 7 m away from the gable wall, and 1 m above the ground; point 3: 108 m away from the east wall, 8 m away from the gable wall, and 0.7 m above the ground), and the carbon dioxide uniformity at these points were observed and analyzed, as shown in Fig. 17 to Fig. 19.

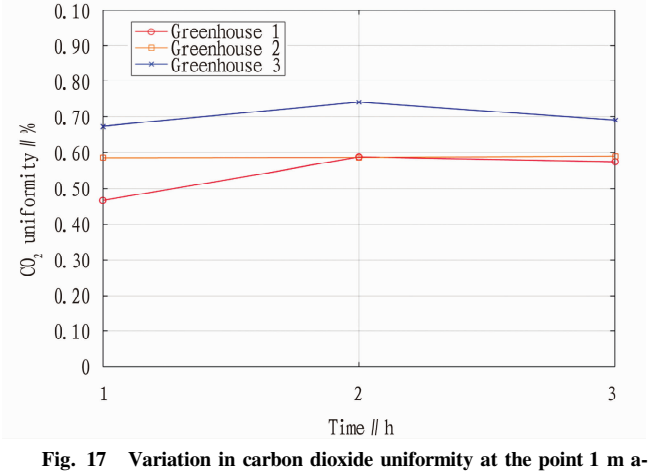

Fig. 17 Variation in carbon dioxide uniformity at the point 1 m away from the east wall, 1 m away from the gable wall and 0.5 m above the ground in the three greenhouses

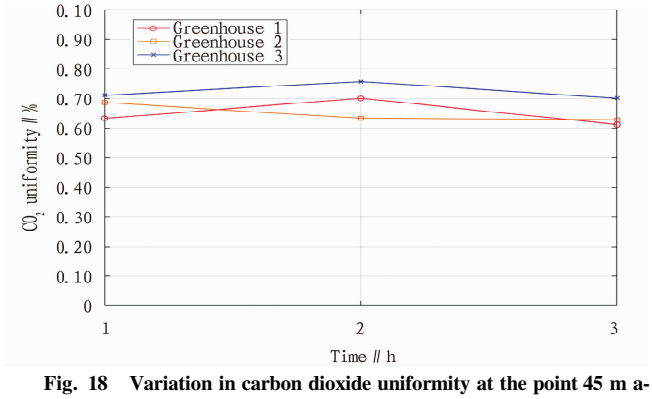

Fig. 18 Variation in carbon dioxide uniformity at the point 45 m away from the east wall, 7 m away from the gable wall and 1 m above the ground in the three greenhouses

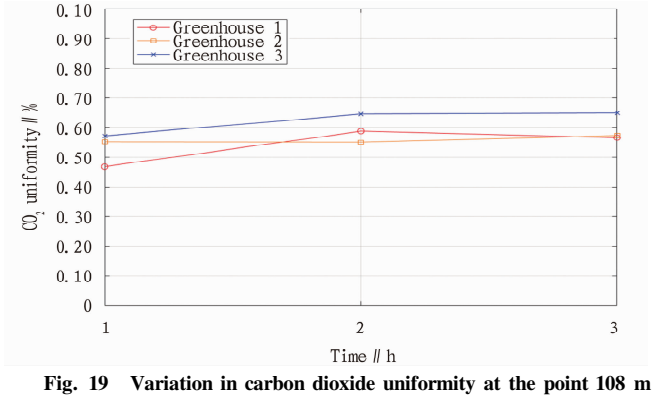

Fig. 19 Variation in carbon dioxide uniformity at the point 108 m away from the east wall, 8 m away from the gable wall and 0.7 m above the ground in the three greenhouses

From the three images above, it can be observed that the uniformity of carbon dioxide concentration in greenhouse 1 fluctuated significantly over the 3 h period, with a noticeable decline in carbon dioxide uniformity during the final stage of carbon dioxide release. It indicated that the placement of the carbon dioxide release device in greenhouse 1 was less than ideal, as it could not consistently and stably provide the required carbon dioxide concentration. In contrast, greenhouse 3 performed well in the first 2 h of carbon dioxide release, but over time, the carbon dioxide concentration gradually decreased, with a relatively large drop. Greenhouse 2 showed the best stability in carbon dioxide concentration. Throughout the 3 h monitoring period, the carbon dioxide concentration in greenhouse 2 remained at a relatively high level with minimal fluctuations. It suggested that the placement of the carbon dioxide release device in greenhouse 2 was the most optimal, as it ensured both uniform distribution of carbon dioxide and a consistent supply of the required carbon dioxide concentration for plant growth. Consequently, the placement position of the carbon dioxide release device in greenhouse 2 was determined to be the best. This location not only guaranteed uniform carbon dioxide distribution but also consistently and stably provided the necessary carbon dioxide concentration for plants throughout the monitoring period, thereby facilitating plant growth and development.

Conclusions and Discussion

In this study, the effects of the placement position of carbon dioxide release devices within greenhouses on airflow distribution and carbon dioxide utilization efficiency were deeply explored, providing a scientific basis for the sustainable development of facility agriculture. Through Ansys Fluent simulation, the internal airflow distribution of the greenhouses under different release positions was analyzed in detail. The results indicated that the placement position of carbon dioxide release devices significantly influenced the internal flow field within the greenhouses, thereby affecting the diffusion and distribution characteristics of carbon dioxide, as well as the uniformity and stability of the greenhouse environment. To determine the optimal position for carbon dioxide release devices, factors such as greenhouse structure, ventilation methods and crop layout were comprehensively considered in this study. Through comparison and analysis on the airflow distribution and carbon dioxide utilization efficiency at different positions, it was found that at the optimal position, the carbon dioxide release device could maximize its effectiveness, improve carbon dioxide utilization efficiency, and create more favorable environmental conditions for crop growth. This finding is of significant guiding importance for environmental regulation and crop growth management in facility agriculture.

In summary, following conclusions were drawn in this study:

(1) Through simulation and theoretical analysis, it was found that the airflow velocity inside greenhouses directly determined the diffusion and distribution of carbon dioxide. Specifically, when the airflow velocity was higher, carbon dioxide could diffuse more uniformly throughout the greenhouse space, effectively increasing the internal carbon dioxide concentration and providing an ample carbon source for plant photosynthesis. Conversely, when the airflow velocity was lower, the diffusion of carbon dioxide was restricted, leading to excessively high or low carbon dioxide concentration in local areas, thereby affecting photosynthetic efficiency and crop growth.

To optimize the distribution of carbon dioxide within greenhouses, the effects of placing carbon dioxide release devices at different positions on carbon dioxide uniformity was compared in this study. Through precise data collection and processing, it was found that the placement position of carbon dioxide release devices significantly influenced the internal airflow distribution and carbon dioxide concentration distribution. Specifically, placing carbon dioxide release devices at a location where laminar flow gathered inside greenhouses could effectively promote airflow circulation and uniform carbon dioxide distribution. In contrast, placing release devices at the lower part or corners of greenhouses tended to cause carbon dioxide accumulation in local areas, reducing carbon dioxide utilization efficiency.

In future academic research, the optimization and improvement of the design and application strategies for carbon dioxide release devices should become a core focus. Precise experiments and simulation analyses are needed to determine the optimal layout and configuration of carbon dioxide release devices within greenhouses to maximize their positive impact on plant growth and yield. Furthermore, with the rapid development of information technology, integrating advanced technologies such as the Internet of Things (IoT) and big data into the environmental management of facility agriculture is particularly necessary. Real-time and accurate perception of the greenhouse environment can be achieved by deploying intelligent sensor networks, and data analysis can guide the formulation of environmental regulation strategies. Such intelligent management approach not only improves resource utilization efficiency and reduces waste, but also provides strong support for the sustainable development of facility agriculture.

References

[1] VANTHOOR BHE, STANGHELLINI C, VAN HENTEN EJ, *et al.* A methodology for model-based greenhouse design: Part 1, a greenhouse climate model for a broad range of designs and climates[J]. Biosystems Engineering, 2011, 110(4): 363 – 377.

[2] CAO GY, HAZIM AWBI, YAO RM, *et al.* A review of the performance of different ventilation and airflow distribution systems in buildings[J]. Building and Environment, 2014, 73: 171 – 186.

[3] YANG-CHENG SHIH, CHENG-CHI CHIU, OSCAR WANG. Dynamic airflow simulation within an isolation room[J]. Building and Environment, 2007, 42(9): 3194 – 3209.

[4] LEUNG DYC, CARAMANNA G, MAROTO-VALER MM. An overview of current status of carbon dioxide capture and storage technologies[J]. Renewable and sustainable energy REviews, 2014, 39: 426 – 443.

[5] TEITEL M, ZISKIND G, LIRAN O, *et al.* Effect of wind direction on greenhouse ventilation rate, airflow patterns and temperature distributions [J]. Biosystems Engineering, 2008, 101(3): 351 – 369.

[6] TAKESHI KUROYANAGI, KEN-ICHIRO YASUBA, TADAHISA HIGASHIDE, *et al.* Efficiency of carbon dioxide enrichment in an unventilated greenhouse[J]. Biosystems Engineering, 2014, 119: 58 – 68.

(Continued on page 82)

Water quality index levels

The water quality index (WQI) was calculated for various monitoring sites in different months using a multi-parameter weighting method. The WQI values were classified into five grades: excellent water quality (WQI < 50), good water quality ($50 \leqslant$ WQI < 100), poor water quality ($100 \leqslant$ WQI < 200), very poor water quality ($200 \leqslant$ WQI < 300), and water unsuitable for drinking (WQI $\geqslant$ 300). Fig. 2 shows the heatmap for monthly WQI distribution at various sampling points throughout the year.

The overall distribution results indicated generally good water quality conditions in the study area. Statistical analysis revealed that 90.77% of samples fell into the "excellent water quality" category, demonstrating that the vast majority of sampling points maintained safe water quality indexes in different seasons. Samples classified as "good water quality" accounted for 6.15% and were primarily concentrated at local monitoring points such as W2 and W3, reflecting the local time periods of pollution interference. Notably, no samples were categorized as "poor water quality" or worse, indicating that the underground river system maintains strong environmental carrying capacity under current climatic and land-use conditions. Additionally, the data missing ratio was 3.08%, primarily caused by sampling vacancies due to equipment failures at individual sampling points or extreme rainfall/drought conditions, which did not significantly affect the representativeness of the assessment results.

The figure further reveals that monitoring points W2 and W3 represented high-value zones, frequently exhibiting WQI values > 50 (classified as "good water quality"). Notably, some monthly values approached or exceeded 90 (*e.g.*, W3 in January, May, and November; W2 in November). These elevated values might be correlated with point-source pollution from domestic wastewater discharge, transportation hubs, or high-density tourist areas upstream. Point W5 also showed a mild water quality decline (WQI = 53.7) in November, suggesting certain organic matter accumulation or non-point source scouring residue during the post-flood season.

Temporally, some monitoring points showed slightly elevated WQI values during the rainy season (May-October), suggesting that stormwater runoff or surface flow may enhance pollutant transport into the underground river system. Particularly during August – November, significant water quality fluctuations at W2 and W3 indicated potential risks arising from combined effects of rainfall and land-use changes. In contrast, other monitoring points (W11-W13) in hydrologically stable mid-downstream areas maintained excellent water quality throughout the year, with WQI consistently below 30.

Conclusions and Discussion

The results of single-factor pollution index demonstrated that TP, NH_4^+-N, NO_3^--N and NO_2^--N maintained clean levels overall, while COD_{Mn} exhibited certain organic pollution characteristics. The Nemerow index analysis revealed that the upstream pollution was greater than the downstream pollution. In upstream areas, the water quality ranged from clean to severely polluted, with lightly polluted samples predominating (50.9%), and the downstream samples were mainly within clean to lightly polluted levels, indicating overall better water quality and limited upstream pollution impacts on downstream areas.

The multi-index evaluation involving WQI demonstrated generally favorable water quality conditions in river basin, with over 90% of samples classified as "excellent water quality". Local water quality deterioration was observed only at upstream monitoring points including W2 and W3 during late rainy seasons or low-water periods, revealing vulnerabilities driven by land use and precipitation in specific areas.

In summary, the Huanghou Underground River Basin maintained overall water quality within the "slightly polluted to good" range, and the pollution was primarily concentrated in upstream areas.

References

[1] NOREEN BEG, MORLOT JAN-CORFEE, DAVIDSON OGUNLADE, *et al.* Linkages between climate change and sustainable development[J]. Climate Policy, 2002, 2(2): 129 – 144.

[2] NICOLAS GRUBER, GALLOWAY JAMES-N. An Earth-system perspective of the global nitrogen cycle[J]. Nature, 2008, 451(7176): 293 – 296.

[3] MA CM, ZHAO LH, LIU CF, *et al.* Advances of the research of isotopic analysis technology for nitrate in natural water[J]. Geotechnical Investigation & Surveying, 2010, 38(7): 37 – 41. (in Chinese).

[4] BATSAIKHAN UURIINTUYA, ZSOLT DARVAS, RAPOSO. People on the move: Migration and mobility in the European Union[J]. Archive of European Integration, 2018, 190.

[5] PACHECO FAL, SANCHES FERNANDES LF. Environmental land use conflicts in catchments: A major cause of amplified nitrate in river water [J]. Science of The Total Environment, 2016: 548 – 549.

[6] LI JY. Basic characteristics of formation and development of karst underground water system in Dushan, Guizhou[J]. Journal of Guizhou University of Technology, 1981(3): 77 – 95. (in Chinese).

Editor: Yingzhi GUANG Proofreader: Xinxiu ZHU

(Continued from page 79)

[7] LAMRANI MA, BOULARD T, ROY JC, *et al.* SE—structures and environment: AirFlows and temperature patterns induced in a confined greenhouse[J]. Journal of Agricultural, 2001, 78(1): 75 – 88.

[8] CHENG JCP, KWOK HHL, LI ATY, *et al.* Sensitivity analysis of influence factors on multi-zone indoor airflow CFD simulation[J]. Science of The Total Environment, 2021, 761: 143298.

[9] VAN HENTEN EJ, BONTSEMA J, VAN STRATEN G. Improving the efficiency of greenhouse climate control: An optimal control approach [J]. Quarterly Journal of the Royal Netherlands Society for Agricultural Sciences, 1997, 45(1).

[10] DONGDONG MA, NEAL CARPENTER, HIDEKI MAKI, *et al.* Greenhouse environment modeling and simulation for microclimate control[J]. Computers and Electronics in Agriculture, 2019, 162: 134 – 142.

Editor: Yingzhi GUANG Proofreader: Xinxiu ZHU